inter.noise
HAMBURG 2016

Vibration-based localisation of structural deterioration in frame-like civil engineering structures

Martin D. ULRIKSEN[1] and Lars DAMKILDE[2]
Department of Civil Engineering, Aalborg University, Niels Bohrs Vej 8, 6700 Esbjerg, Denmark

ABSTRACT
With the existing trend of minimising material use in typical frame-like civil engineering structures, such as buildings, bridges, and offshore platforms, these structures will typically be subjected to substantial wind-induced vibrations. Besides being a source of disturbance for the occupants, these vibrations can potentially lead to an evident risk of structural deterioration. In order to ensure the safety of the structures, it is thus paramount that the potential structural deterioration can be identified before it becomes critical from a structural integrity point of view. One way of facilitating such identification is by use of structural health monitoring (SHM) techniques, which enable remote, typically through pre-installed sensors, diagnosing of the structural health. In the present paper, it is examined whether a vibration-based SHM approach proposed by the authors—and previously applied successfully to other structural systems, for instance, wind turbines—can provide reliable damage localisation in frame-like structures. The performance of the method, which is based on statistical interrogation of changes in a surrogate of the transfer matrix, is tested in a Monte Carlo setting with a numerical steel frame model subjected to white noise excitation.

Keywords: Structural health monitoring, Vibration analysis, System identification, Damage localisation.
I-INCE Classification of Subjects Number: 42.

1. INTRODUCTION

By inspection of typical civil engineering structures, it is evident that many of these are, basically, more or less complex frame-like structures. This holds, as examples, for bridges, offshore platforms, and different types of residential, commercial, and industrial buildings. In the ongoing attempt to minimise material use, these frame-like structures are now designed less conservative, which inherently reduces the safety margins towards failure. Equivalently, the risk of structural deterioration increases, hence implying the need for more frequent structural integrity inspections.

Today, structural integrity inspections of most civil engineering structures are primarily conducted based on visual and manual approaches, which can be very tedious and costly. Furthermore, the manual aspect subjects the outcome of the inspection to human decision-making, which adversely precludes a unequivocal procedure. Therefore, these structures constitute prime candidates for being subjected to structural health monitoring (SHM). This is, of course, widely acknowledged in the SHM research community, where numerous studies concerning different types/steps of damage identification—that is, damage detection, localisation, assessment, and/or consequence evaluation [1]—have been carried out. Common for the majority of these studies is the use of vibration signals as the feature from which the structural integrity is decided. In principle, the structure is potentially damaged if the vibration signals, aggregated into some more or less advanced mathematical feature, of the current state differ significantly from those captured from the (typically) healthy reference state.

[1]Email: mdu@civil.aau.dk
[2]Email: lda@civil.aau.dk

In [2], a numerical model of a three-dimensional frame structure is successfully studied in the context of damage localisation and assessment. The damage identification is conducted through a Cross-Modal Strain Energy (CMSE) method that is based on solving simultaneous equations involving quantities equivalent to modal strain energy (MSE) terms for the baseline (healthy) structure and the damaged counterpart. The MSE terms are computed from the modal parameters, particularly, the eigenfrequencies and mode shapes, thus the method inherently requires identification of these. A damage localisation method that does not require identification of the modal parameters is tested in [3]. Here, the applicability of the Damage Location Vector (DLV) method [4], which is based on interrogating changes in the structure's flexibility for damage localisation, is examined in an experimental context with a three-dimensional frame. The results suggest that the method has merit, albeit few of the introduced damages are not localised.

The DLV method employed in the experimental study in [3] has been extended to a dynamic approach (the DDLV method [5]), which, again, has been formulated for the stochastic case where the input is unknown (the SDDLV method [6]). In the present study, we apply an outlier analysis-based extension of the SDDLV method to localise damage in a numerical model of a two-dimensional frame structure that, very simplistic, emulates a frame-like civil engineering structure. The latter methodological extension was, in a slightly modified version, originally proposed by the authors in [7]. Yet, for the sake of completeness, the theoretical principles and their specific composition in the method are reviewed in a condensed form in sections 2 to 4. Subsequently, the application example is treated in section 5, and, lastly, some concluding remarks are stated in section 6.

2. STRUCTURAL MODELLING

We recall that the transfer matrix, $G(s) \in \mathbb{C}^{n\times n}$, of the linear, time-invariant (LTI) dynamical system with n degrees of freedom (DOF) is given by

$$G(s) = (Ms^2 + Cs + K)^{-1} \Rightarrow \mathbf{X}(s) = G(s)\mathbf{F}(s), \tag{1}$$

where $M, C, K \in \mathbb{R}^{n\times n}$ are the mass, damping, and stiffness matrices, while $\mathbf{X}(s) = \mathcal{L}(\mathbf{x}(t))$ and $\mathbf{F}(s) = \mathcal{L}(\mathbf{f}(t))$ are the Laplace transforms of the displacement output and load input, respectively.

In those cases where only the output is available, as will be the premise in this study, the input in time domain is assumed to be white Gaussian noise. If one additionally assumes that the measurements are collected in l coordinates, and that the unmeasured load is converted into fictive forces acting exclusively in these l coordinates, the receptance transfer matrix, $G(s) \in \mathbb{C}^{l\times l}$, can be expressed as [6]

$$G(s) = Z(s)B_c, \tag{2}$$

with

$$Z(s) = C_c A_c^{-b}(sI - A_c)^{-1} \in \mathbb{C}^{l\times m}. \tag{3}$$

Here, $b = 0$, 1, or 2 (depending on whether displacements, velocities, or accelerations are measured), while $A_c \in \mathbb{R}^{m\times m}$, $B_c \in \mathbb{R}^{m\times l}$, and $C_c \in \mathbb{R}^{l\times m}$ are the state transition matrix, the input matrix, and the output matrix, respectively, from the continuous state-space realization

$$\begin{cases} \dot{\mathbf{y}}(t) = A_c\mathbf{y}(t) + B_c\mathbf{u}(t) \\ \mathbf{d}(t) = C_c\mathbf{y}(t) + D_c\mathbf{u}(t) \end{cases} \tag{4}$$

of model order m. $\mathbf{y} \in \mathbb{R}^{m\times 1}$ is the state vector, $\mathbf{d} \in \mathbb{R}^{l\times 1}$ is the output vector, $\mathbf{u} \in \mathbb{R}^{l\times 1}$ is the fictive input force acting only in the measured coordinates, and $D_c \in \mathbb{R}^{l\times l}$ is the direct input-output transmission matrix. Estimates of A_c and C_c can be obtained by use of standard output-only system identification techniques, for

instance, stochastic subspace identification (SSI), see [8]. However, due to the lack of known input, B_c and D_c cannot be identified directly. In [6], the relation

$$HB_c = LD_c \Rightarrow B_c = H^{\dagger}LD_c \quad \forall m \leq 2l \tag{5}$$

is derived with the constraint $m \leq 2l$, because this modal truncation ensures that the pseudo-inverse yields an unique solution [6]. In Eq. (5), † denotes the Moore-Penrose pseudo-inverse and

$$H = \begin{bmatrix} C_c A_c^{1-b} \\ C_c A_c^{-b} \end{bmatrix} \in \mathbb{R}^{2l \times m}, \quad L = \begin{bmatrix} I \\ 0 \end{bmatrix} \in \mathbb{R}^{2l \times l}, \tag{6}$$

thus by plugging the explicit expression for B_c in Eq. (5) into Eq. (2), one gets

$$G(s) = Z(s)H^{\dagger}LD_c. \tag{7}$$

3. (S)DDLV METHOD

The DDLV method is based on a theorem stating that the span of the null space of the change in the transfer matrix, ΔG, contains vectors that are Laplace transforms of excitations for which the dynamic stress field is identically zero over the portion of the structure where the damage is located [5].

Adhering to the case of unknown input, this realization of the transfer matrix is impossible. In [6], Bernal proposes a stochastic extension of the DDLV method—termed the SDDLV method—in which a surrogate of ΔG is interrogated. Using ~ to denote the damaged state and omitting the references to the Laplace variable for simplicity, ΔG can be written as

$$\Delta G = \tilde{G} - G = \tilde{Z}\tilde{H}^{\dagger}L\tilde{D}_c - ZH^{\dagger}LD_c = \tilde{D}_c^T\tilde{R}^T - D_c^T R^T, \tag{8}$$

where

$$R = ZH^{\dagger}L. \tag{9}$$

If ones makes the (often reasonable) assumption that the stiffness is the system parameter pre-dominantly influenced by structural damages, it holds that $\text{null}(\Delta G) \approx \text{null}(\Delta R^T)$, as D_c is independent of K. Hereby, $\text{null}(\Delta G)$ can be obtained from the singular value decomposition (SVD)

$$\Delta R^T = U\Sigma V^H = \begin{bmatrix} U_1 & U_2 \end{bmatrix} \begin{bmatrix} \Sigma_1 & 0 \\ 0 & \Sigma_2 \end{bmatrix} \begin{bmatrix} V_2 & V_2 \end{bmatrix}^H, \tag{10}$$

where, theoretically, $\Sigma_2 = 0$. It is noticed, however, that in practice, $\Sigma_2 > 0$ due to noise and other disturbances, thus, from this perspective, the vectors in $V_2 \subset V = [\mathbf{v}_1, \mathbf{v}_2, \ldots, \mathbf{v}_l]$ constitute quasi-null vectors with potential as load vectors. By selecting $\mathbf{v}_l = \mathbf{v}_l(s)$ as the load vector, the displacements in Laplace domain can be computed as

$$\mathbf{X}(s) = G_{\text{model}}(s)\mathbf{q}_l(s), \tag{11}$$

where $\mathbf{q}_l \supseteq \mathbf{v}_l$ is expanded with zeros to all DOF and $G_{\text{model}} \in \mathbb{C}^{n \times n}$ is the transfer matrix of the reference state mechanical model, which, in this study, is obtained from a finite element (FE) model.

From the displacements computed via Eq. (11), the stresses can readily be obtained. As the SDDLV theorem states [6], these stresses will, theoretically, approach zero in the domain where damage is located. In practice, studies have shown—see, for example, [7, 9, 10]—that it becomes troublesome to discriminate

between damaged elements and healthy ones when noise and other disturbances are present. Consequently, a statistical enhancement is employed.

4. STATISTICAL INTERROGATION OF STRESS FIELDS

4.1 Outlier analysis

Consider the baseline, training matrix $\Phi_{\text{tr},j} \in \mathbb{R}^{k\times\alpha}$, whose k rows are constituted of α elemental mean von Mises stresses from element j in the healthy structural state. Here, α corresponds to the number of chosen s-values in the SDDLV approach.

In order to discard information that is of no use for damage localisation, $\Phi_{\text{tr},j}$ is transformed into a latent variable subspace

$$T_j = \Phi_{\text{tr},j} P_j \tag{12}$$

by use of principal component analysis (PCA). T_j and P_j contain, respectively, the principal component scores (emphasising the variation in $\Phi_{\text{tr},j}$) and the principal components (constituting the axes in the new, principal coordinate system). With the aim of deriving an uncorrelated, orthogonal basis, it can be shown, see, for instance, [11], that

$$\Sigma_j P_j = P_j \Lambda_j, \tag{13}$$

where Σ_j is the covariance matrix of $\Phi_{\text{tr},j}$. Thus, the principal components, P_j, are found as the eigenvectors of Σ_j, while the variance associated with each principal component is the corresponding eigenvalue contained in $\Lambda_j = \text{diag}(\lambda_{1,j}, \lambda_{2,j}, \ldots, \lambda_{\alpha,j})$.

Testing the stresses in element j in the current state—gathered in $\boldsymbol{\phi}_{\text{te},j} \in \mathbb{R}^{1\times\alpha}$—is done through the Mahalanobis metric

$$D_j^2 = \left(\boldsymbol{\phi}_{\text{te},j} - \overline{\boldsymbol{\phi}}_{\text{tr},j}\right) \acute{P}_j \acute{\Lambda}_j^{-1} \acute{P}_j^T \left(\boldsymbol{\phi}_{\text{te},j} - \overline{\boldsymbol{\phi}}_{\text{tr},j}\right)^T, \tag{14}$$

where $\acute{P}_j \subseteq P_j$, $\acute{\Lambda}_j \subseteq \Lambda_j$ constitute the chosen principal component basis and $\overline{\boldsymbol{\phi}}_{\text{tr},j}$ is the vector mean of $\Phi_{\text{tr},j}$. $\boldsymbol{\phi}_{\text{te},j}$ is then labelled as outlier or inlier on the basis of the following hypothesis formulation:

$$\left.\begin{array}{l} H_{0,j} : D_j^2 \leq \vartheta_j \\ H_{1,j} : D_j^2 > \vartheta_j, \end{array}\right\}, \tag{15}$$

in which $H_{0,j}$ implies that no anomalies are present in the jth element, while $H_{1,j} = \neg H_{0,j}$ indicates damage in this particular element.

The threshold, ϑ_j, is found through the training data in an exclusive manner. Here, a Mahalanobis distance between each row in $\Phi_{\text{tr},j}$ and the remaining k-1 rows is calculated, and subsequently the k D_j^2-metrics are sorted in a descending order. Finally, ϑ_j is then chosen as the value exceeded by $5\ \%$.

4.2 On selecting pole(s) for interrogation

The fundamental idea of the presented damage localisation method is to interrogate ΔR^T for damage-induced changes in the vicinity of one or more system pole(s). When a pole has been chosen for inclusion in the damage localisation, specific s-values close to this pole are appointed.

Findings in [7] suggest that selecting ten s-values equally spaced with $1\ \%$ of the real part of a pole is a proper basis for the statistical evaluation when they are placed on a "right side"-tangent to the exclusionary circle defined in [5, 6]. This circle criterion excludes s-values that belong to the interior of a circle that is centred at the identified pole, $\lambda_i^{(p)}$, and has a radius of $0.125\ \omega_i$. In Figure 1, the uncertainties associated with estimation of the first pole of the frame structure treated in section 5—estimated from a Monte Carlo procedure with 250 simulations and subsequent system identification—are presented for the case of $5\ \%$

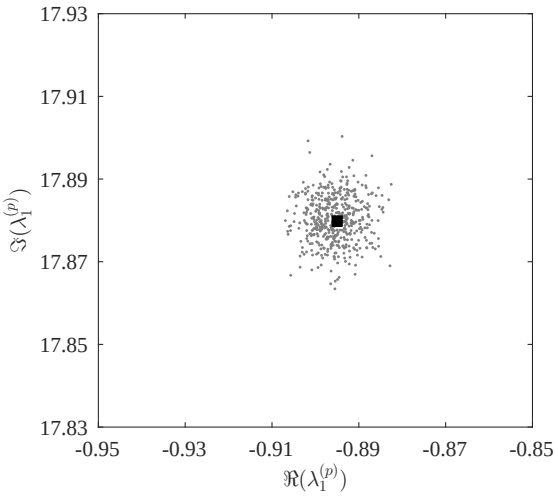

Figure 1. Simulated uncertainties of first pole of the considered frame model (see Figure 2).

white Gaussian noise added to the output. These uncertainties form a circular pattern, which reveals that it is reasonable to assume that the variance for $\Re(\lambda_i)$ is equal to that of $\Im(\lambda_i)$. Thus, from an estimation point of view, it does not seem to matter which tangent to the exclusionary circle we select. Additionally, it is also seen that since $\omega_1 = 17.90$ rad/s, the radius of the exclusionary circle is 2.24 rad/s, thus the uncertainties are clearly bounded by this.

When determining whether a particular pole should be selected for inclusion, one can refer to the sensitivity to damage of the system's eigenspace. In this respect, we consider the undamped eigenvalue formulation of the system described by Eq. (1), whose derivative with regard to some variable z is

$$\left(\frac{\partial K}{\partial z} - \frac{\partial \gamma_i}{\partial z} M - \gamma_i \frac{\partial M}{\partial z}\right)\boldsymbol{\psi}_i + \left(K - \gamma_i M\right)\frac{\partial \boldsymbol{\psi}_i}{\partial z} = 0, \tag{16}$$

where γ_i and $\boldsymbol{\psi}_i$ are, respectively, the distinct undamped eigenvalue and the undamped eigenvector of the i'th mode. For mass-normalised eigenvectors, pre-multiplication with $\boldsymbol{\psi}_i^T$ yields

$$\boldsymbol{\psi}_i^T \left(\frac{\partial K}{\partial z} - \gamma_i \frac{\partial M}{\partial z}\right)\boldsymbol{\psi}_i - \frac{\partial \gamma_i}{\partial z} = 0, \tag{17}$$

in which it is assumed that structural deterioration merely affects the stiffness. Consequently, z is chosen as a region in the stiffness matrix, termed k_k, such

$$\frac{\partial \gamma_i}{\partial k_k} = \boldsymbol{\psi}_i^T \frac{\partial K}{\partial k_k}\boldsymbol{\psi}_i \Rightarrow \frac{\partial \omega_i}{\partial k_k} = \frac{1}{2\omega_i}\boldsymbol{\psi}_i^T \frac{\partial K}{\partial k_k}\boldsymbol{\psi}_i, \tag{18}$$

which enables quantification of the eigenfrequency sensitivities towards stiffness changes in each single region. The same procedure goes for the eigenvector, hence

$$\frac{\partial \boldsymbol{\psi}_i}{\partial z} = -\left(K - \gamma_i M\right)^- \frac{\partial K}{\partial k_k}\boldsymbol{\psi}_i, \tag{19}$$

where the generalized inverse [12]

$$\left(K - \gamma_i M\right)^- = \Psi\left(\Gamma - \gamma_i I\right)^\dagger \Psi^T \tag{20}$$

is employed since $\left(K-\gamma_i M\right)$ is rank deficient. In Eq. (20), $\Gamma \supset \gamma_i$ and $\Psi \supset \boldsymbol{\psi}_i$ are, respectively, a diagonal matrix containing the eigenvalues and a matrix containing the eigenvectors in its columns.

As evidenced, the product $\boldsymbol{\psi}_i^T \frac{\partial K}{\partial k_k} \boldsymbol{\psi}_i$ governs the sensitivities. In this way, one can identify suitable poles to use if prior knowledge is available regarding, for example, at which location/area damage is predominantly likely to occur, or at which pole(s) the global sensitivity to the damage is high. While prior knowledge of the likelihood of damage occurring at specific locations is seldom available, the global sensitivity towards the damage can in fact be quantified for each of the identified poles—or a subset of poles if these are very closely coupled—as a subsequent part of the damage *detection* procedure. The reader is referred to [7] for more information on this procedure.

5. APPLICATION EXAMPLE

To examine the applicability of the proposed method for localising damages in frame-like civil engineering structures, we consider the 8 m high and 4 m wide two-dimensional steel frame model depicted in Figure 2. The frame, which is assigned an isotropic material model corresponding to regular construction steel, is subjected to scaled white Gaussian noise excitation in nodes 13-20 (showed with arrows), and the resulting horizontal displacements are captured in the nodes that are coloured red with a sampling frequency of 100 Hz. Classical damping is assumed such each mode has a damping ratio of $\zeta_i = 5\ \%$.

5.1 FE modelling and simulations

As seen in Figure 2, a simplistic model (composed of two-dimensional Bernoulli-Euler beam elements) is chosen in this preliminary applicability study. Besides the obvious simplification with regard to spatial dimensionality, it is also assumed that the kinematic boundary conditions are fixed, thus no soil-structure interaction is taken into account. This simplistic approach is chosen, as we recall that the purpose of this

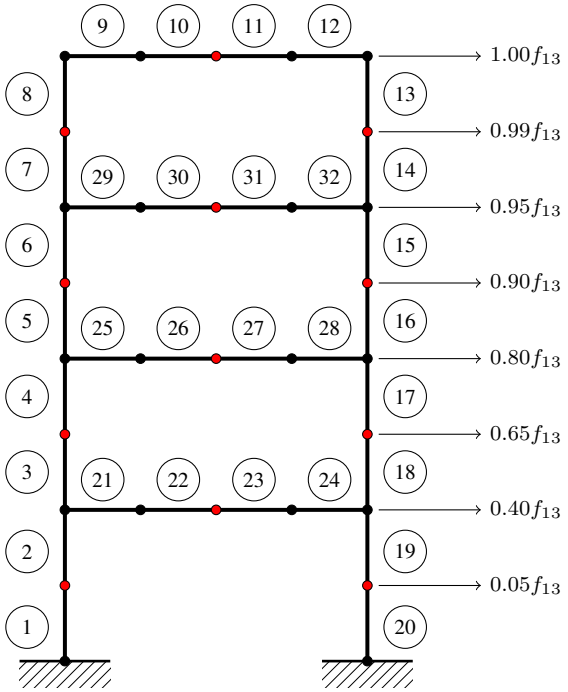

Figure 2: Considered frame structure with element numbering. The overall width of the frame is 4 m, while the height is 8 m.

Table 1: Eigenfrequencies for the first three modes of the frame structure in structurally healthy and damaged configurations.

Mode	Eigenfrequency (Hz) (healthy)	Eigenfrequency (Hz) (damaged)
1	2.8492	2.8456
2	9.5453	9.5283
3	18.4674	18.4591

particular study is to examine the preliminary potential of the presented method. Thus, if the method fails at locating the damage in this study, it is unlikely that it will facilitate useful results when the system becomes more complex.

In order to simulate damage, the modulus of elasticity for beam element 4, see Figure 2, is reduced with $10\ \%$. In Table 1, the first three eigenfrequencies of, respectively, the healthy configuration and the damaged one are presented. These particular modes are selected, as they compose those that often are most realistic to obtain in an operational context. As seen in Table 1, the damage induces relatively small changes in the treated eigenfrequencies.

For each of the two structural configurations, a Monte Carlo procedure with 250 simulations is carried out with white Gaussian noise excitation, applied as depicted in Figure 2, to yield displacement output samples, which are corrupted with $5\ \%$ white Gaussian noise to emulate real experimental findings. Subsequently, a subspace-based output-only system identification technique is used to identify the state-space matrices A_c and C_c needed for damage localisation.

5.2 Damage localisation

Previous research by the authors [7] reveals that ten s-values equally spaced—with $1\ \%$ of the real part of a pole—constitutes an auspicious basis for the statistical evaluation when these s-values are selected on the particular "right side"-tangent to the exclusionary circle that is parallel to the imaginary axis. Consequently, this configuration is chosen in the vicinity of the poles of modes 1, 2, and 3. Recalling the discussion on the selection of s-values, see subsection 4.2, the assumption of damaged being smeared across an entire element precludes direct damage insensitivity for any mode, even though node 5 is nearly a nodal point of mode 3.

Through the Monte Carlo simulations, 250 surrogates of the transfer function matrix change for, respectively, healthy-healthy and healthy-damaged combinations have been computed, hereby resulting in a total of 7,500 von Mises stress fields for each of the two combination types due to the configuration with 10 s-values around each pole. Of the 250 healthy-healthy combinations, the first 150 are used for training the baseline model (including the threshold for each element), thus $\Phi_{\text{tr},j} \in \mathbb{R}^{150\times 30}$. By use of PCA, $\Phi_{\text{tr},j} \mapsto \acute{T}_j \in \mathbb{R}^{150\times 3}$, that is, only the three first principal component scores are utilized, as these have been found to account for $99\ \%$ of the variance in $\Phi_{\text{tr},j}$.

For testing, the remaining 100 stress vectors from the healthy-healthy combinations are used along with the 250 from the healthy-damaged combination. The final results for the two structural states are seen in Figures 3 and 4, where the probability of detecting (POD) anomalies in each element is presented. That is, the percentage scale expresses the number of realisations that yields a Mahalanobis metric exceeding the threshold relative to all realisations available for testing in the particular state. Thus, if an element is assigned a value of $100\ \%$, it indicates that the Mahalanobis metrics calculated for this element all exceed the threshold.

As evidenced in Figure 3, only a few type I errors, that is, false damage classifications, are obtained when interrogating the change in transfer matrix surrogate in a healthy-healthy context. The few type I errors are, of course, expectable because of the probabilistic nature of the threshold computation, in which we have used $\vartheta_j = 5\ \%$. For the damaged configuration, element 4 is correctly labelled as damaged in $97\ \%$ of the

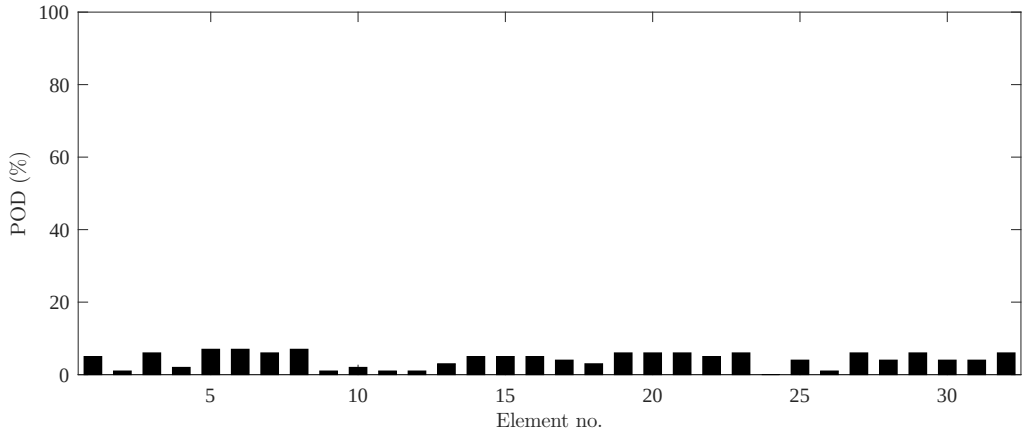

Figure 3. Percentage damage classification in the healthy testing state.

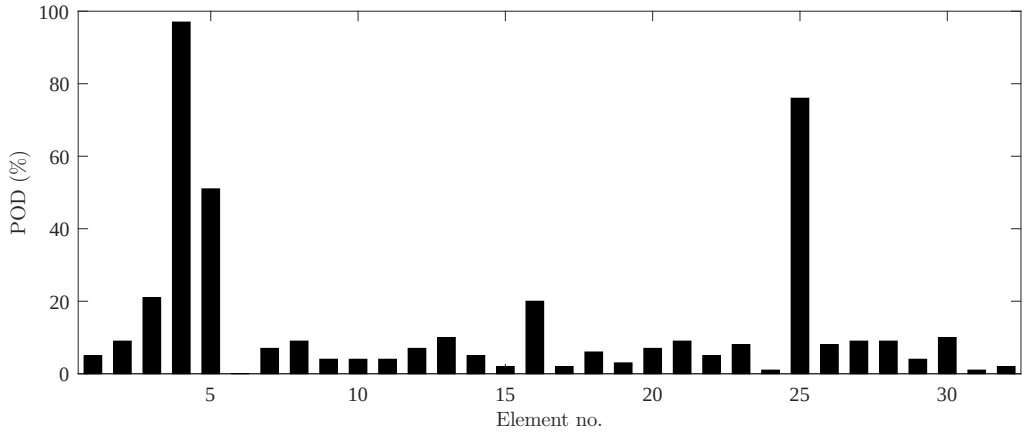

Figure 4. Percentage damage classification in the damaged testing state.

realisations, while the adjacent elements—that is, number 3, 5, and 25—also frequently are labelled as being damaged. From a practical point of view this is, however, not a major drawback.

6. CONCLUSION

The present paper deals with damage localisation in a numerical frame model that, in a very simplistic manner, emulates a frame-like civil engineering structure. Based on Monte Carlo simulations with this model in both undamaged and damaged states, it has been shown how an outlier analysis-based extension of the SDDLV method facilitates valid localisation of the introduced damage. It is, however, also noted that the employed approach frequently labels the elements adjacent to the damaged one as being damaged.

It is paramount to stress that, in general, the study presented is of very simplified nature, but due to the promising results herein, the main part of the future work will be to treat more realistic conditions; including soil-structure interaction, different loading types (wind, waves, etc.), more advanced modelling of the damage, and the effect of sensor type and placement.

ACKNOWLEDGEMENTS

The authors of the paper would like to show their gratitude to the European Union for financial support via the Interreg V project “Urban Tranquility”.

REFERENCES

[1] A. Rytter. *Vibration Based Inspection of Civil Engineering Structures*. PhD thesis, Aalborg University, 1993.

[2] H. Li, H. Fang, and S.-L. J. Hu. Damage localization and severity estimate for three-dimensional frame structures. *Journal of sound and Vibration*, 301(3-5):481–494, 2007.

[3] B. Gunes and O. Gunes. Structural health monitoring and damage assessment Part ii: Application of the damage locating vector (dlv) method to the asce benchmark structure experimental. *International Journal of Physical Sciences*, 7:1509–1515, 2012.

[4] D. Bernal. Load vectors for damage localization. *Journal of Engineering Mechanics*, 128(1):7–14, 2002.

[5] D. Bernal. Damage localization from the null space of changes in the transfer matrix. *AIAA Journal*, 45(2):374–381, 2007.

[6] D. Bernal. Load vectors for damage location in systems identified from operational loads. *Journal of Engineering Mechanics*, 136(1):31–39, 2010.

[7] M.D. Ulriksen, D. Tcherniak, L.M. Hansen, R.J. Johansen, L. Damkilde, and L. Frøyd. In-situ damage localization for a wind turbine blade through outlier analysis of sddlv-induced stress resultants. *Submitted to Strucutural Health Monitoring*, 2016.

[8] P. v. Overschee and B. De Moor. *Subspace identification for linear systems: theory - implementation - applications*. Kluwer Academic Publishers, 1 edition, 1996.

[9] Luciano Marin, Michael Döhler, Dionisio Bernal, and Laurent Mevel. Robust statistical damage localization with stochastic load vectors. *Structural Control and Health Monitoring*, 22(3):557–573, 2015.

[10] R.J. Johansen, L.M. Hansen, M.D. Ulriksen, D. Tcherniak, and L. Damkilde. Damage localization in a residential-sized wind turbine blade by use of the sddlv method. *J. Phys.: Conf. Ser.*, 628(1):012069, 2015.

[11] S. Sharma. *Applied Multivariate Techniques*. John Wiley & Sons, 1995.

[12] J.R. Magnus and H. Neudecker. *Matrix differential calculus with applications in statistics and econometrics*. John Wiley & Sons, 2nd edition, 1999.